16C.8 A SYNTHETIC TRAPPED-FETCH WAVE CLIMATOLOGY FOR THE NORTH ATLANTIC AND EASTERN PACIFIC

Allan W. MacAfee *
National Lab for Marine and Coastal Meteorology, Meteorological Service of Canada

1. INTRODUCTION

Tropical cyclones (TCs) that generate extreme ocean waves in midlatitudes (e.g., Luis 1995; Danielle, 1998; Juan 2003) exhibit two common features: the TC traveled in a straight line for at least 18 h and the speed exceeded 10 m s^{-1}. As explained in Bowyer and MacAfee (2005, hereafter BM5), these conditions result in a trapped-fetch wave (TFW) situation whereby the significant wave height (H_{SIG}) can become much greater than for waves generated by a stronger but slower moving TC.

A Lagrangian TFW model based on the significant wave method and driven by a parametric wind model is described in MacAfee and Bowyer (2005, hereafter MB5). The wind model inputs are TC track and intensity data and a number of model-specific parameters such as radius of maximum winds. Values for these model-specific parameters are obtained using statistical procedures outlined in MacAfee and Pearson (2006). After interpolating the track to hourly positions, a local wind grid aligned along the instantaneous TC motion vector is defined and computed at each hourly position. The full set of wind grids is then fed to the TFW model which outputs dominant wave trajectories for each grid. This TFW model is used operationally at the Canadian Hurricane Centre to predict extreme wave events with TCs affecting Atlantic Canada.

Similarly, using TC historical data from the National Hurricane Center's hurricane database archive (HURDAT, Jarvinen et al. 1984) and the parameter-setting statistical procedures, hourly wind fields can be defined along any historical TC, then fed to the TFW model.

Creation of the TFW database is outlined in section 2. Display tools, creation of supplementary datasets, and some recommended applications are discussed in sections 3 and 4. A summary in section 5 completes the paper.

2. METHODOLOGY

The modeling procedure outlined above was used for the 1324 North Atlantic (NA) TCs from 1851–2004 and the 767 Eastern Pacific (EP) TCs from 1949–2003. For each TC, a plain-text file of TFW data was generated containing the grid definition at each interpolated hourly track point and data for the dominant TFW from each right-of-track row within the grid as illustrated graphically in Fig. 1. Further details on the grid and modeling procedures are found in MB5.

* *Corresponding author address*: Allan W. MacAfee Meteorological Service of Canada, 45 Alderney Drive, Dartmouth, NS, Canada B2Y 2N6
e-mail: Al.MacAfee@ec.gc.ca

The TFW data consists of hourly values of the wave point's latitude and longitude, H_{SIG} (m), wave period (T_P; s), length or distance over which growth occurred (n mi; 1 n mi = 1.852 km), the duration or elapsed time (h) during which TFW growth occurred to reach that point, and the angle (^{o} True) of the trajectory.

Prior to 1950, TCs were unnamed and assigned numbers. In this study the numeric numbering system has been replaced by letters (e.g., R 1933).

Several post-processing procedures were developed to mine the TFW output. These methods are discussed and illustrated in section 4.

3. TFW DISPLAY TOOL

Fig. 1 illustrates ***climviewer***, a Graphical User Interface (GUI) designed for easy display of individual TCs and their TFWs. Although only one TC can be viewed at a time, multiple TCs can be loaded. Four TCs named Floyd are listed, but Floyd 1999 is displayed.

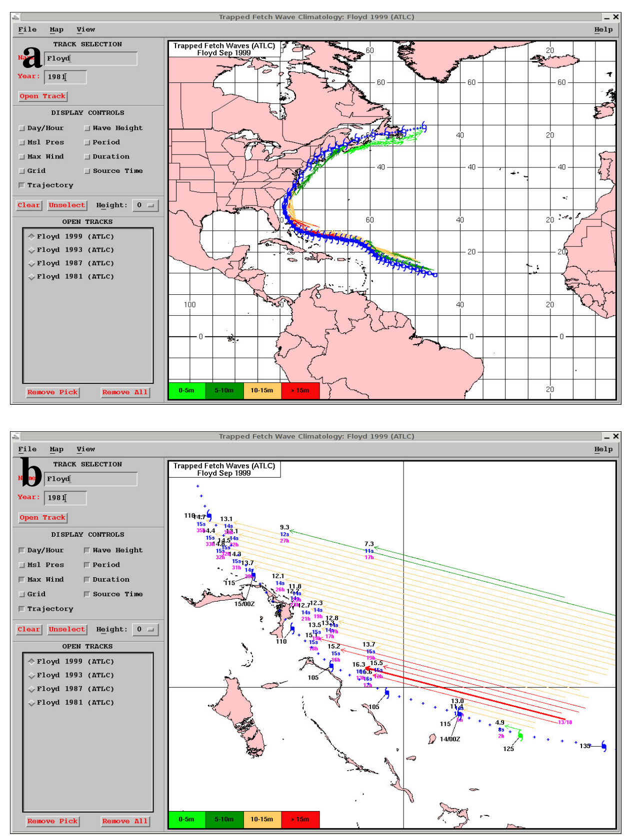

FIG. 1. Examples of ***climviewer*** – GUI used to view the TFW database: (a) dominant TFWs along the track of Floyd 1999; (b) zoomed view of TFWs generated from a specific track point grid (highlighted in green).

Selecting a TC in the list quickly displays the database information. Attributes for the TC (e.g., maximum wind at 6-h positions) can be displayed using the various toggle buttons on the GUI. These labels can be dragged to new locations on the map to improve readability.

In addition to the visual indication of the distance covered during the time of TFW growth, numeric values of H_{SIG}, T_P, and the number of hours of TFW growth can be added to the display. In the zoomed view in Fig. 1b, the dominant TFW from each row of the 1600 UTC 13 September 1999 grid are displayed; the track point is highlighted in green.

The map view can be saved in a PNG-format file for further study and inclusion in reports.

.

4. DATABASE APPLICATIONS

4.1 *Risk Assessment*

To create a risk potential dataset, the NA trajectories for the 100-year period 1905–2004 and the EP trajectories for the 50-year period 1954–2003 were sorted into 2^o x 2^o latitude cells. Using the latitude and longitude of each hourly position along a given trajectory, each position was assigned to a cell. The H_{SIG}, T_P, length, duration, and angle were then sorted into bins and counters incremented accordingly. The bin intervals were: H_{SIG} 1 m, T_P 1 s, duration 1 h, length 5 n mi, and angle 5^o. If successive hourly positions on the same trajectory fell in the same cell, the position with the highest wave growth was recorded ignoring the earlier positions and values. In addition, the name, year, and highest wave height for each TC contributing to any given cell were recorded on a cell by cell basis.

The cell-bin counts of H_{SIG}, T_P, length, duration, and angle as well as each contributing TC (name, year, and cell-specific maximum H_{SIG}) were recorded in a plain-text file.

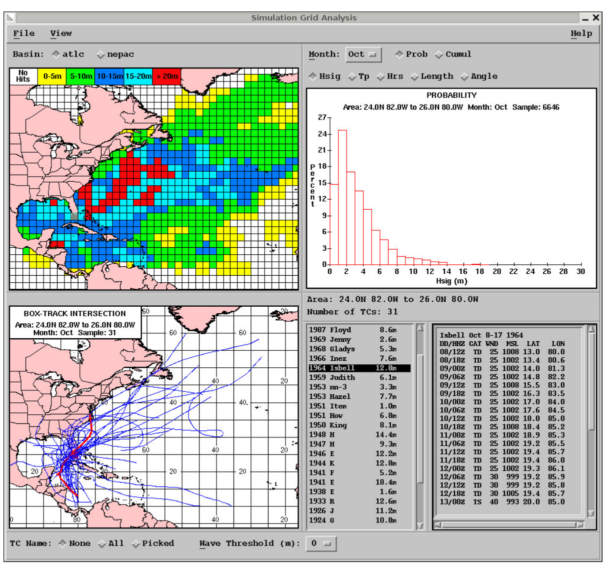

FIG. 2. Example of ***chart*** – GUI for viewing the cell analysis.

Fig. 2 shows the display program ***chart***, a GUI used to access the cell analyses. In addition to the basin and month switches, the color-coded cells (upper left panel) are selectable. Clicking on a cell fills the remaining panels with cell-specific information: frequency diagrams (upper right); the list of contributing TCs (lower right) with the TC contributing the highest H_{SIG} automatically highlighted and its track data displayed; tracks of all contributing TCs (lower left) with the TC contributing the highest H_{SIG} highlighted in a thicker red line. The track map can be annotated with TC names. The number of displayed tracks can be reduced by setting a minimum wave height threshold.

Each map can be zoomed and panned. The map views and probability diagrams can be saved in PNG-format files for further study and inclusion in reports.

Frequency diagrams are available for H_{SIG}, T_P, hours of wave growth, distance covered during wave growth, and TFW direction. Figs. 3 and 4 show a selection of these diagrams for October for the cell, highlighted in gray, on the southwest tip of Florida. On the TFW direction radial plot (Fig. 4b), the direction contributing the highest wave to the cell is highlighted in a thicker red line which, in this example, is not the most frequently occurring direction.

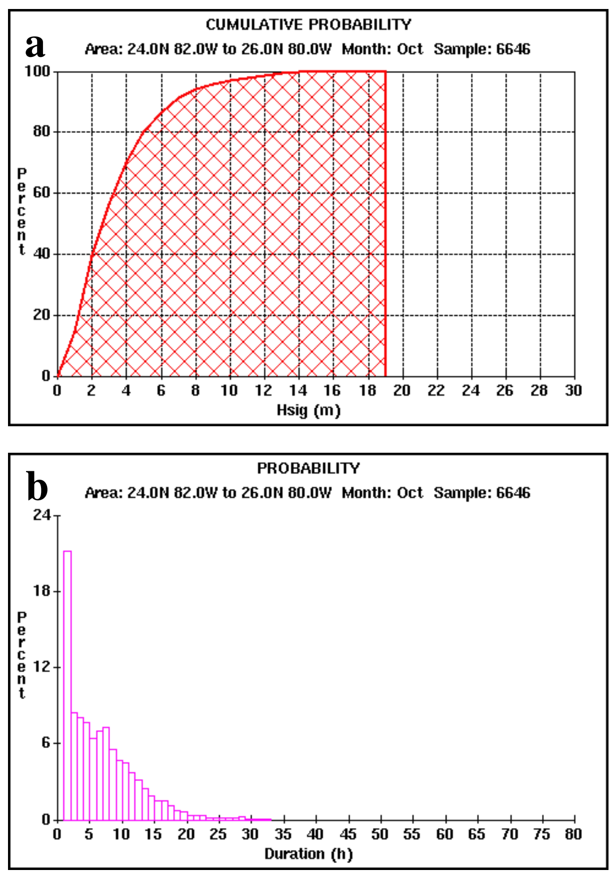

FIG. 3. Example of ***chart*** probability diagrams: (a) cumulative H_{SIG}; (b) hours of growth leading to the wave position in the cell.

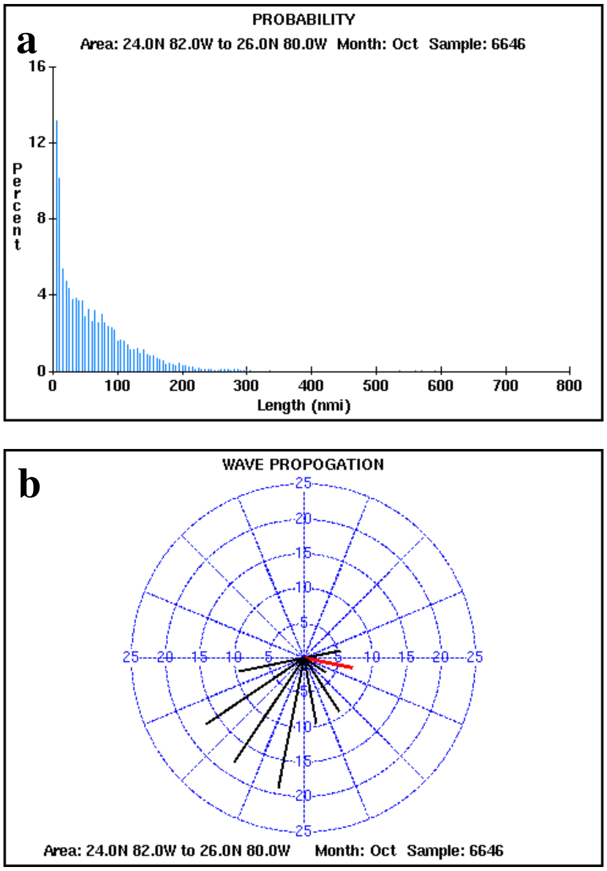

FIG. 4. Same as Fig. 3 except: (a) distance the wave traveled to its final position in the cell; (b) direction frequency.

4.2 *Extreme Waves*

Consider mining the TFW dataset, for extreme events such as waves 25 m or higher. One approach uses ***chart*** to examine the list of contributing TCs for cells with 15 m or higher. This is a reasonable approach if interested only in a specific geographical location, but tedious on a basin wide examination. A second approach directly examines the raw TFWs and extracts TCs with any TFW exceeding a threshold.

Using the 100-year NA and 50-year EP storms and a 20 m threshold, 83 extreme events were identified in the NA and 16 in the EP basins.

In the NA basin, 15 TCs generated TFWs of 25 m or higher (Table 1) with individual tracks and dominant TFWs shown in Appendix A. These TCs are distributed across the basin and have different track orientations and intensities. Nonetheless, they exhibit one common feature: in agreement with BM5, the highest TFWs for each TC were when the storm was moving in a straight line for at least 18 hours with intensity and translation speed appropriately linked.

In the EP, none of the TCs in the 50-year period generated TFWs of 25 m or higher, but five TCs generated at least 23 m (Table 2; Appendix B). Qualitatively, as shown in Appendix B, the top four extreme TFW TCs are similar in intensity, track orientation, and translation speed.

TABLE 1. NA TCs generating TFW ≥ 25 m.

Year	Name	H_{SIG} (m)	T_P (s)	Hours	Length (n mi)
1922	B	36.1	24.0	33	906
1982	Debby	32.0	22.7	34	900
1933	R	29.3	21.6	18	449
1952	Charlie	28.0	21.1	39	938
1938	D	27.6	20.5	24	528
1956	Greta	27.0	20.9	39	1011
1916	D	27.0	20.7	26	573
2004	Alex	26.5	20.8	34	807
1948	G	26.1	20.6	41	966
1932	D	25.9	20.4	20	478
1963	Flora	25.8	20.5	48	1132
1951	Fox	25.3	20.1	23	516
1955	Janet	25.2	19.5	10	223
1954	Hazel	25.2	20.0	25	552
1980	Allen	25.1	20.0	20	452

TABLE 2. EP TCs generating TFW ≥ 23 m.

Year	Name	H_{SIG} (m)	T_P (s)	Hours	Length (n mi)
1994	John	24.2	19.1	36	682
1983	Raymond	23.9	19.3	29	625
1973	Ava	23.8	19.1	31	629
1986	Estelle	23.6	19.1	18	396
1982	Olivia	23.3	19.2	33	631

4.3 *Supplement to* AES40

The methodology, output, and validation of a 40-Year (1958–97) Wave Hindcast for the Atlantic (AES 40) is described in Swail et al. (2000a,b). The wave model used in AES40 was driven by kinematically reanalysed wind fields. As outlined in Swail et al. (2000b), particular attention was given to adjustments to TC wind fields by using high-resolution surface wind fields from a TC boundary layer model (Thompson and Cardone 1996). As noted in MB5, TFWs represent one spectral mode and, given an accurate wind field, a full-spectral wave model should capture the TFWs generated by the significant wave method. Hence, within limits, the AES40 database should contain information on TFW extremes. As an application example, Wang and Swail (2002) used the AES40 to study trends in extreme waves.

The highlighted area on Fig. 5 denotes the Sable marine forecast area. Fig. 6 shows the AES40 H_{SIG} frequency for October, generated by the Atlantic Climate Centre, averaged over the Sable area. The frequency of H_{SIG} over 8 m is less than 1%.

The NA trajectories from 1958–97 affecting the marine areas of Fig. 5 were determined using the sorting technique described earlier substituting polygons for grid cells. From this analysis, 731 TFWs from 9 TCs were recorded in the Sable area of which 6% exceed 8 m (Fig. 6). Similarly, for the 100-year period, 2123 TFWs from 15 TCs were recorded in the Sable area of which 25% exceed 8 m with the highest TFW 17 m (R 1933).

These cursory comparisons suggest that using the TFW climatology enhances detection of important wave events beyond that provided by the AES40 hindcast.

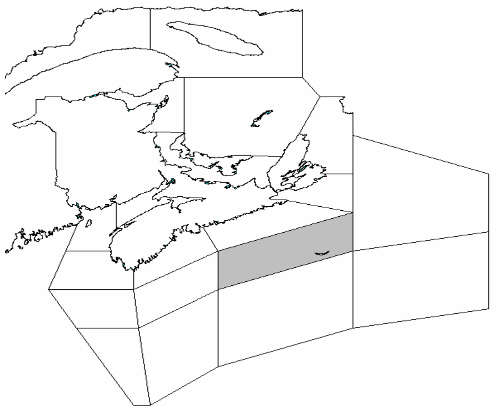

FIG. 5. Sable forecast area (highlighted)

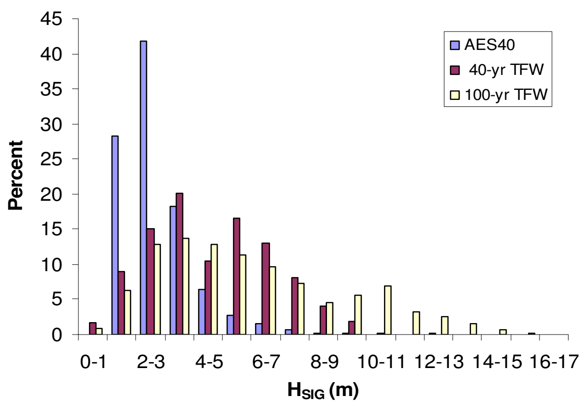

FIG. 6. H_{SIG} frequencies for the Sable marine area using different sources.

4.4 ***Analog Searching***

During the real-time prediction of Wilma (2005), the operational TFW model indicated 16 m waves near the southwest coast of Florida (Fig. 7a). Using ***chart***, a cell near the area of interest was selected: the highlighted (gray) cell in Fig. 2.

From the list of contributing TCs, Isbell (1964) was identified as having a similar track to Wilma and generating TFWs near 12 m (Fig. 7b). The maximum TFWs for Wilma were predicted prior to crossing Florida while Isbell's maximum TFWs were over the NA after crossing Florida. The variation in location of the highest TFWs is due to the rapid acceleration of Wilma after crossing Florida versus a more gradual acceleration for Isbell, consistent with the TFW theory outlined in BM5.

This example illustrates that TFW information from historically similar TCs may assist in evaluating forecast scenarios for real-time storms.

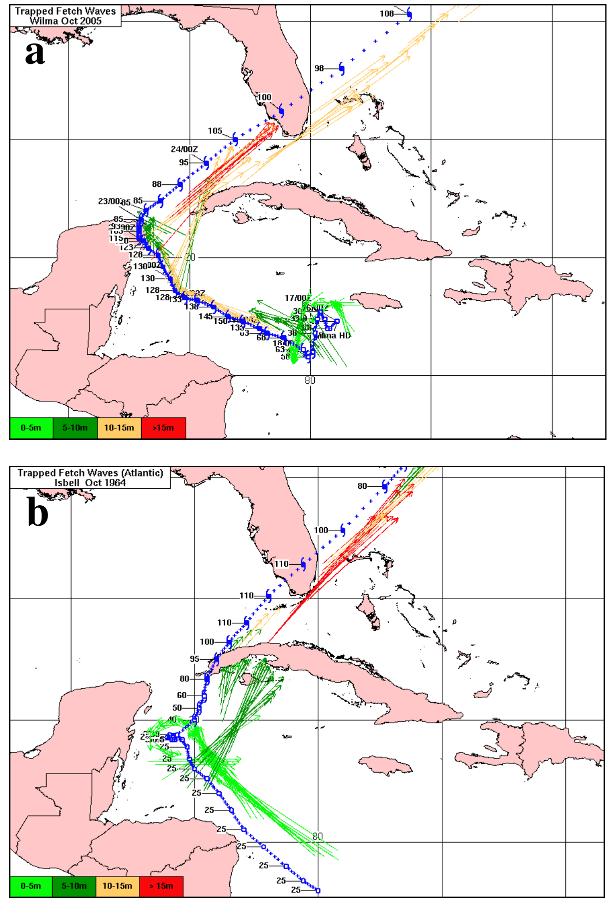

FIG. 7. Dominant TFWs for (a) Wilma (2005) and (b) Isbell (1964).

4.5 ***Track and Intensity Reanalyses***

On 10–11 September 1995, Hurricane Luis passed approximately 222 km northwest of buoy 44141 (42.07°N, 56.15°W) near the time of the arrival of a 17.1 m H_{SIG}. The TFW climatology shows 9–11 m waves between buoy 44141 and the storm track and 9 m at the buoy. These wave heights were 50–70% of the maximum H_{SIG} reported at buoy 44141. The HURDAT dataset for Luis shows winds of 51 m s^{-1} before recurvature and 44 m s^{-1} immediately after, but Jones et al. (2003) stated that some transitioning TCs do not weaken following recurvature. Luis' speed was over 23 m s^{-1} as it passed buoy 44141. From Fig. 12 of BM5, storms moving in excess of 21 m s^{-1} require a wind well in excess of 51 m s^{-1} to develop large TFWs. As shown in MB5, increasing the maximum winds after recurvature generated TFWs in closer agreement to buoy data.

This example illustrates that the TFW climatology may be useful in identifying TCs where the intensity and/or speed produce waves inconsistent with observation.

The list of extreme waves in Tables 1 and 2 may be used as a starting point in selecting storms for re-examination. Are the 36.1 m TFW from B 1922 and the

32.0 m TFW from Debby 1982 reasonable? From Appendix A, the tracks are very similar and present the signatures expected for significant TFW growth (BM5). Debby is further north with the maximum TFW growth reached at 46.2°N 50.9°W, just southeast of Newfoundland in a well-trafficked marine fishing area. The maximum TFW from B 1922 reached its maximum growth at 40.4°N 52.8°W becoming decaying swell brushing the outermost marine area southeast of Newfoundland. B 1922 was the more intense storm with the 36.1 m TFW originating from an intensity of 67 m s^{-1}. Debby's 32.0 m TFW began from a 51 m s^{-1} intensity. As shown in BM5, storm speed was critical to the development of these extreme TFWs. Because of the proximity to active marine areas, further examination of these TCs may be in order.

4.6 *Long-term Trend Analyses*

To create long-term trend analyses datasets, the 100-year (50-year) periods (section 4.1) were used. Along each trajectory, the successive hourly values of H_{SIG} were examined and when H_{SIG} crossed a critical threshold (3 m intervals to 27 m), H_{SIG} bin counters and variables to determine T_P, length, and duration means and standard deviations were incremented. The extracted threshold data were then sorted by Julian day and year. The output of these analyses were written to file in comma-delimited format for access and further processing by spread-sheet programs (e.g., Excel) as illustrated in Fig. 8.

TABLE 3. TFW H_{SIG} occurrence for each basin.

H_{SIG} (m)	NA Number	NA Percent	EP Number	EP Percent
3	2654806	65.82	1889290	66.64
6	1285097	31.86	980922	34.60
9	588793	14.60	417352	14.72
12	233925	5.80	149885	5.29
15	77693	1.93	46308	1.63
18	19234	0.48	13040	0.46
21	4010	0.10	2242	0.08
24	477	0.01	2	0.00
27	74	0.00	0	0.00

Table 3 lists the NA and EP percentage of TFWs for the H_{SIG} thresholds. For example, of the NA 4,033,194 wave growth points, only 1.93% were ≥ 15 m and 0.1% ≥ 21 m.

Using normalized 5-year running means and linear regression analyses, some interesting observations will be presented; detailed statistical analyses are beyond the scope of this paper.

1) NORTH ATLANTIC

The normalized 5-year running means and linear regression analyses for the yearly TFW totals for thresholds from 3 to 15 m are shown in Fig. 8. The normalization consisted of converting each yearly total, for a particular H_{SIG} threshold, to a percentage of the highest year total during the 100-year period. Since

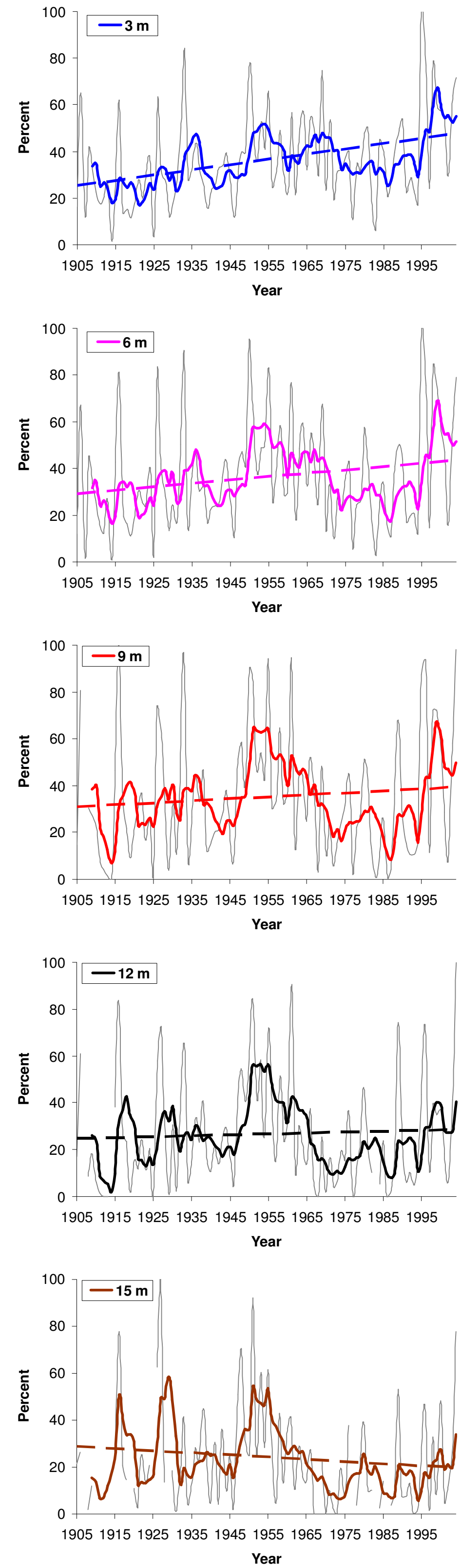

FIG. 8. Normalized running means (solid heavy line) and linear regression (dashed line) for NA basin TFW H_{SIG} thresholds of 3, 6, 9, 12, and 15 m.

the number of events diminished with Increasing threshold height (Table 3), this normalization facilitated inter-comparison of different thresholds. The linear regression analysis was performed for each threshold using the normalized yearly-sorted data. It should be noted that regression correlation coefficients are small (< 0.1).

The 3, 6, 9, and 12 m trends are upward, but with decreasing regression line slope with increasing threshold. Beyond 12 m, there is a slight decreasing trend with little slope variation towards higher heights. From these trends, it is inferred that the number of individual TCs has increased or individual TCs are persisting longer or there is some combination of increased number and increased persistence. Thus, overall, TC activity is increasing; however, the occurrence of conditions favorable for extreme TFW growth is not linked to increased activity.

2) NORTHEAST PACIFIC

The normalized 5-year running means and linear regression analyses for the yearly TFW totals for thresholds from 3 to 15 m are shown in Fig. 9.

The trend for all wave height thresholds is upward. The slope of the regression line decreases only slowly with increasing threshold. Hence, it is inferred that overall TC activity is increasing. The occurrence of conditions favorable for extreme TFW growth is positively linked to increased TC activity.

5. SUMMARY

A Lagrangian TFW model based on the significant wave method and driven by a parametric wind model has shown utility in predicting extreme waves associated with TCs. Because the model inputs are track positions and intensities and statistical estimates of wind model parameters, it's possible to compute TFWs for historical storms.

All TCs in the period 1851–2004 in the NA basin and 1948–2003 in the EP were modeled and available for viewing on an individual basis. The 100-year (50-year) period 1905–2004 (1954–2003) was extracted from the NA (EP) database to investigate potential uses of the TFW data: risk assessment, extreme wave detection, long-term trend analyses, and analog searching.

Case studies have shown that TFW model output, in conjunction with wave information, may be useful in detecting historical TCs where the track and intensity generate TFWs not in agreement with observation.

6. REFERENCES

Atlantic Climate Centre, 2003: Marine Atlas – Atlantic Coast (1958–1997): AES40 Dataset. Environment Canada, Fredericton, NB.

Bowyer, P. J. and MacAfee, A. W., 2005: The Theory of trapped-fetch waves with tropical cyclones–An operational perspective. *Wea. Forecasting*, **20,** 229–244.

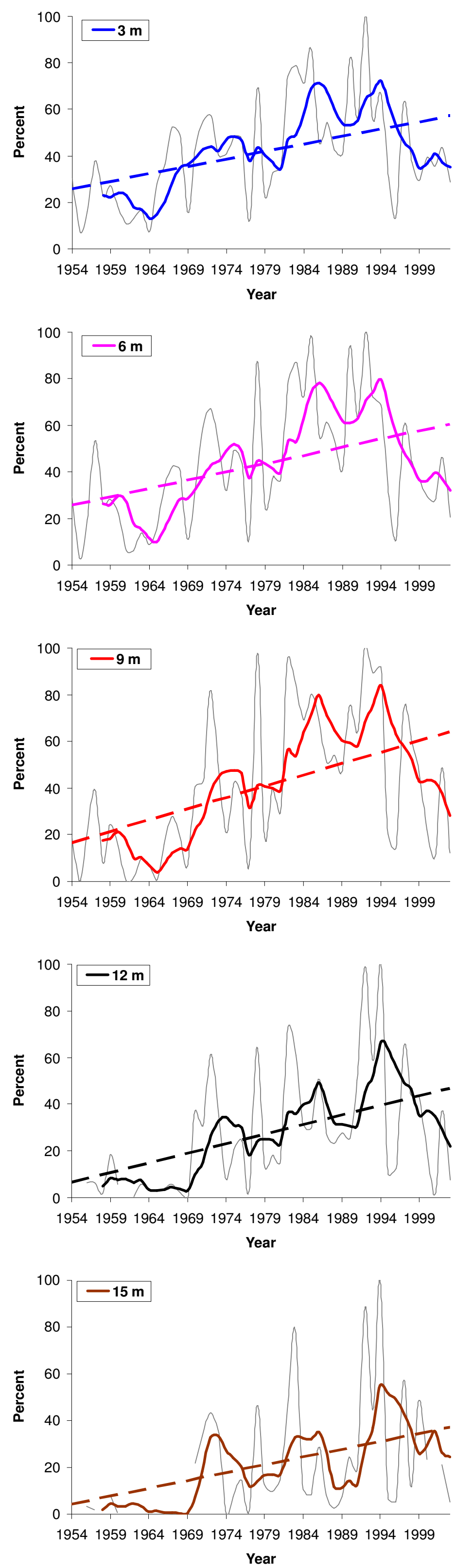

FIG. 9. Same as Fig. 8 except EP.

Jarvinen, B. R., C. J. Neumann, and M.A. S. Davis, 1984: A tropical cyclone data tape for the north Atlantic Basin, 1886-1983: Contents, limitations, and uses. NOAA Tech. Memo. NWS NHC 22, Miami, FL, 21 pp.

Jones, S. C., and Coauthors, 2003: The extratropical transition of tropical cyclones: forecast challenges, current understanding, and future directions – review article. *Wea. Forecasting*, **6,** 1052–1092.

MacAfee, A. W., and P. J. Bowyer, 2005: The modeling of trapped-fetch waves with tropical cyclones–A desktop operational model. *Wea. Forecasting,* **20,** 245–263.

———, and G. M. Pearson, 2006: Development and testing of tropical cyclone parametric wind models tailored for mildlatitude application–Preliminary results. Submitted to *J. Appl. Meteor. and Climatol.*

Swail, V. R., E. A. Ceccacci, and A. T. Cox, 2000a: The AES40 North Atlantic wave reanalysis: Validation and climate assessment. *Proc. 6th Int.Workshop on Wave Hindcasting and Forecasting*, Monterey CA, USA, 1–15.

———, and A. T. Cox, 2000b: On the use of NCEP/NCAR reanalysis surface marine wind fields for a long-term North Atlantic wave hindcast. *J. Atmos. Oceanic Technol.,* **17,** 532–545.

Thompson , E. F., and V. J. Cardone, 1996: Practical modeling of hurricane surface wind fields. *J. Waterway, Port, Coastal, Ocean Eng.*, **112 (4),** 195–205.

Wang, X. L., and V. R. Swail, 2002: Trends of Atlantic wave extremes as simulated in a 40-yr wave hindcast using kinematically reanalyzed wind fields. *J. Climate,* **15,** 1020–1034.

APPENDIX A

Tracks and Dominant TFW for the Extreme North Atlantic Events

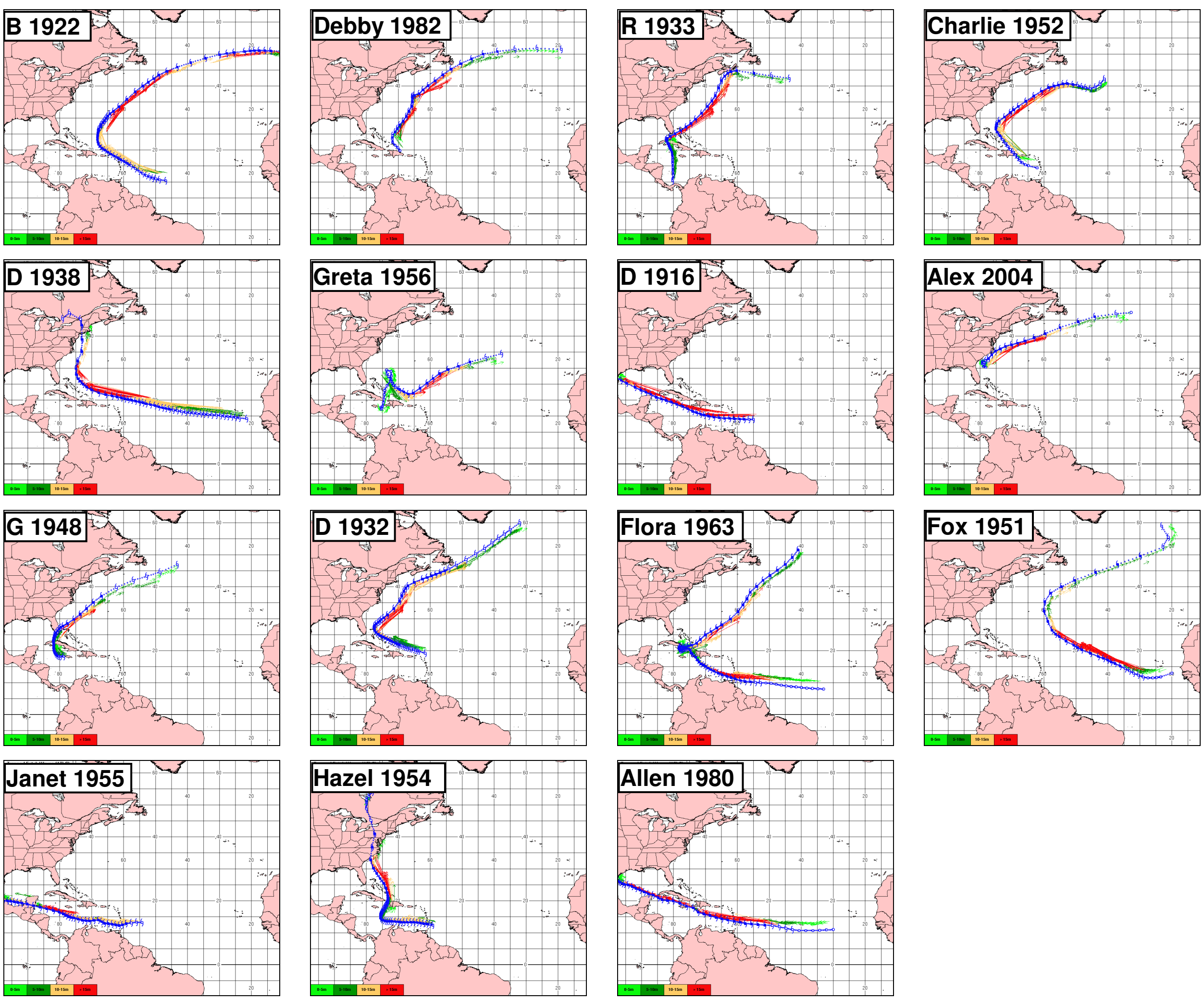

APPENDIX B

Tracks and Dominant TFW for the Extreme Eastern Pacific Events